

Typical wheel–rail profile change rules and matching characteristics of high speed railway in China

Characteristics
of wheel–rail
matching

289

Maorui Hou

*Railway Science and Technology Research and Development Center,
China Academy of Railway Sciences Corporation Limited, Beijing, China*

Fengshou Liu

*Metals and Chemistry Research Institute,
China Academy of Railway Sciences Corporation Limited, Beijing, China, and*

Xiaoyi Hu

*Railway Science and Technology Research and Development Center,
China Academy of Railway Sciences Corporation Limited, Beijing, China*

Received 11 January 2022
Revised 28 February 2022
Accepted 20 April 2022

Abstract

Purpose – In order to systematically grasp the changes and matching characteristics of wheel and rail profiles of high speed railway (HSR) in China, 172 rail profile measurement points and 384 wheels of 6 high-speed electric motive unites (EMUs) were selected on 6 typical HSR lines, including Beijing–Shanghai, Wuhan–Guangzhou, Harbin–Dalian, Lanzhou–Xinjiang, Guiyang–Guangzhou and Dandong–Dalian for a two-year field test.

Design/methodology/approach – Based on the measured data, the characteristics of rail and wheel wear were analyzed by mathematical statistics method. The equivalent concity of wheel and rail matching in a wheel reprofiling cycle was analyzed by using the measured rail profile.

Findings – Results showed that when the curve radius of HSR was larger than 2,495 m, the wear rate of straight line and curve rail was almost the same. For the line with annual traffic gross weight less than 11 Mt, the vertical wear of rail was less than 0.01 mm. The wear rate of the rail with the curve radius less than 800 m increased obviously. The wheel tread wear of EMUs on Harbin–Dalian line, Lanzhou–Xinjiang line and Dandong–Dalian line was relatively large, and the average wear rate of tread was about 0.05–0.06 mm·(10,000 km)⁻¹, while that of Beijing–Shanghai line, Wuhan–Guangzhou line and Guiyang–Guangzhou line was about 0.03–0.035 mm·(10,000 km)⁻¹. When the wear range was small, the equivalent concity increased with the increase of wheel tread wear. When the wear range of wheel was wide, the wheel–rail contact points were evenly distributed, and the equivalent concity did not increase obviously.

Originality/value – This research proposes the distribution range of the equivalent concity in one reprofiling cycle of various EMU trains, which provides guidance for the condition-based wheel reprofiling.

Keywords High speed railway (HSR), Typical railway line, Rail wear, Wheel wear, Wheel–rail interface, Equivalent concity

Paper type Research paper

1. Introduction

Due to long mileage of lines, the high proportion of ballastless tracks, complex geological, climatic and environmental conditions, electric motive unite (EMU) trains of different types and speed classes sharing the same tracks, as well as trains continuously running at a high



© Maorui Hou, Fengshou Liu and Xiaoyi Hu. Published in *Railway Sciences*. Published by Emerald Publishing Limited. This article is published under the Creative Commons Attribution (CC BY 4.0) licence. Anyone may reproduce, distribute, translate and create derivative works of this article (for both commercial and non-commercial purposes), subject to full attribution to the original publication and authors. The full terms of this licence may be seen at <http://creativecommons.org/licenses/by/4.0/legalcode>

This research is supported by the China Academy of Railway Sciences Corporation Limited (Grant no. 2019YJ162).

Railway Sciences
Vol. 1 No. 2, 2022
pp. 289-306
Emerald Publishing Limited
e-ISSN: 2755-0915
p-ISSN: 2755-0907
DOI 10.1108/RS-04-2022-0019

speed, the wheel–rail interface is especially complex for high speed railway (HSR) in China. There are 2 types of rail head profiles (60D and 60N) matching with 5 types of wheel treads (LM_A , LM_D , S1002CN, XP55 and LM_B-10). In some sections, typical wheel–rail interaction problems have arisen such as abnormal vibration of bogie frame which exceeds the limit, uneven wear of wheel tread and poor wheel–rail contact patch (Zhou *et al.*, 2017).

For HSR, on the one hand, minor changes in wheel and rail profiles directly affect the train operation safety and ride comfort; on the other hand, changes in wheel and rail profiles are closely related to the maintenance cost of rails and wheels. In recent years, many studies on wheel and rail wear have been conducted in China and other countries. Sawlwy and Wu (2005) studied tread hollow wear and its impact on the dynamic behaviors of freight cars and determined the limit of hollow wear. Polach (2010) studied the characteristics of nonlinear changes in the equivalent conicity curve of wheel–rail matching, proposed 2 evaluation indexes that can reflect the extent of nonlinear changes of the equivalent conicity and analyzed their impact on dynamic behaviors. Wu, Kalay and Tournay (2011) established a wheel–rail interaction management platform based on the wheel–rail profiles measured on site, which can predict such defects as wheel/rail wear and rolling contact fatigue and provide guidance for on-site maintenance. Karttunen, Kabo and Ekberg (2014) studied the impact of tread wear on rail and wheel defects with the numerical method. Based on the matching between new wheels and rails, Sun, Wang, Li and Zheng (2006), Li, Wen and Jin (2008), Zhang, Xiao, Wang and Jin (2009), Zhang, Jin, Sun and Zhang (2010) studied the influence of the matching between various wheel and rail profiles, the distance between backs of wheel rims/flanges, the rail cant and other factors on wheel–rail contact geometry and dynamic behaviors of cars. Gan, Dai, Gao and Wei (2013) analyzed wheel–rail contact characteristics by using 3 equivalent conicity calculation methods for 4 high speed wheel treads, respectively, providing reference for wheel wear analysis. Huang, Cui, Du and Jin (2013) studied the eccentric wear caused by tread hollow wear and its impact on dynamic behaviors of cars, and discovered that the in-phase eccentric wear greatly affected the critical speed and stability of cars. Jin *et al.* (2018) summarized lateral hollow wear conditions of high speed train wheel treads in China and proposed measures in 7 aspects to suppress such wear. All the references above studied the matching between profiles of wheels and TB60 standard rail. Zhou, Tian, Zhang, Chang and Hou (2014a) studied the alarm caused by the lateral vibration acceleration of the frame which exceeded the limit due to too large equivalent conicity of wheel–rail matching of CRH₃ EMU trains. Zhou, Zhang, Tian, Chen, Fiu, Yu and Li (2014b) and Sun (2017) studied the matching between profiles of wheels and 60N rail. Compared with TB60 rail, the wheel 60N contact points are concentrated in the center of rail head and all the dynamic behaviors are better. Dong, Wang, Ren, Wang and Liu (2014) studied the lateral instability (lurching) of carbody caused by too small equivalent conicity of wheel–rail matching of CRH_{3C} EMU trains.

Many previous studies were based on new wheels and new rails while studies on changes in profiles of in-service rails and treads of in-service wheels and their matching characteristics were insufficient. In order to systematically understand the change rules and matching characteristics of wheel and rail profiles of HSR in China, 172 points for measuring changes in rail profiles and 16 high speed EMU trains were selected on 6 typical HSR, including Beijing–Shanghai, Wuhan–Guangzhou, Harbin–Dalian, Lanzhou–Urumchi, Guiyang–Guangzhou and Dandong–Dalian for a two-year field test. As for the selection principle and scheme, refer to Hou *et al.* (2018).

Based on a large number of rail and wheel profiles measured in the field test, this paper analyzes the change rules in rail profiles and wheel profiles of various lines with a modern statistical method and analyzes the equivalent conicity based on the measured rail profiles. In this way, the main characteristics of the wheel and rail profile matching and the difference between various HSR in China are obtained and relevant optimization measures and suggestions are proposed.

2. Changes in rail profiles

Rail profile changes consist of rail grinding (including grinding by large track maintenance machines and quick grinding) and natural rail wear. Refer to [Table 1](#) for changes in rail profiles at different measuring points on various railway lines.

It can be seen from [Table 1](#) that when the influence of rail grinding on changes in rail profiles is not taken into account, the vertical wear of rails is positively correlated with the annual passing tonnage, and for lines with an annual passing tonnage of less than 11 Mt (Harbin–Dalian, Lanzhou–Urumchi, Guiyang–Guangzhou and Dandong–Dalian), the vertical rail wear is close to 0.01 mm, which is beyond the measuring precision of instruments; Rail profile changes significantly due to grinding and the maximum area of changes is 9.30 mm², 90% of which is caused by grinding; Changes in rail profiles vary significantly at the measuring points of different sections due to the difference between grinding processes and methods. In general, the grinding depth of quick grinding is small and that of grinding by large track maintenance machines is large. Changes in rail profiles affect wheel–rail contact and train operation quality. Scientific and reasonable grinding processes should be adopted and grinding quality should be strictly controlled, so as to ensure good wheel–rail contact relationship.

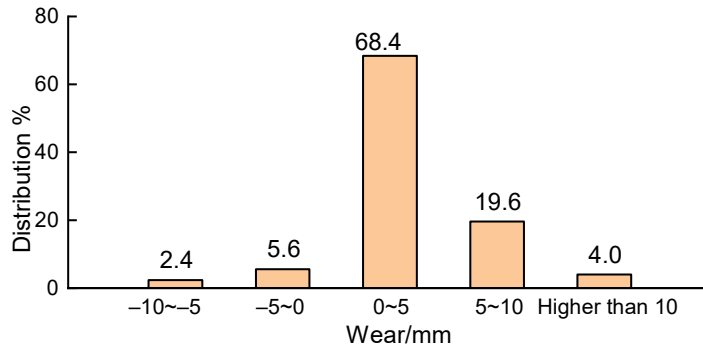
Statistical analysis results of the distribution of maximum rail wear points are shown in [Figure 1](#), where positive values indicate the rail wear towards the gauge corner. [Figure 1](#) shows that 68.4% of the maximum wear points are concentrated in a range from 0 to 5 mm from the rail head center to the working gauge. According to the *Rules on Maintenance of Ballastless Track of High Speed Railway*, vertical rail wear shall be measured at 1/3 of the width of the rail top surface (from the standard working gauge) ([National Railway Administration of the People’s Republic of China, 2018](#)), and for TB60 rails, the measuring

Measuring point	Changes in profiles at vertical wear points/mm		Area of changes in profiles/mm ²		Annual passing tonnage/Mt	Interval/month
	Vertical wear	Grinding depth	Vertical wear	Grinding depth		
Beijing–Shanghai HSR (CR-Beijing)	0.05	0.020*	1.70	1.50*	66.0	21
Beijing–Shanghai HSR (CR-Jinan)	0.03	0	1.41	0	39.4	12
Beijing–Shanghai HSR (CR-Shanghai)	0.04	0	1.28	0	42.0	14
Wuhan–Guangzhou HSR (Shaoguan)	0.04	0.035*	1.15	2.60*	44.0	11
Wuhan–Guangzhou HSR (Xianning)	0.04	0.001 ^Δ	1.20	9.30 ^Δ	45.0	12
Harbin–Dalian HSR (Haicheng)	0.01	0	0.32	0	10.9	13
Lanzhou–Urumchi HSR (CR-Lanzhou)	0.01	0	0.44	0	4.2	12
Lanzhou–Urumchi HSR (CR-Qinghai-Tibet)	0.01	0.030 ^Δ	0.52	3.34 ^Δ	4.2	12
Guiyang–Guangzhou HSR (CR-Chengdu)	0.01	0	0.25	0	6.3	18
Dandong–Dalian HSR (Qianyang)	0.01	0	0.50	0	4.2	19

Note(s): * refers to quick grinding; ^Δ refers to grinding by large track maintenance machines

Table 1.
Statistical results of
changes in rail profiles

Figure 1.
Distribution of
maximum rail wear
positions



points shall be at the 13.5 mm from the rail head center. HSR main lines usually have a large curve radius and vertical wear rarely occurs near the gauge corner. Therefore, it is recommended to measure the vertical wear at 5 mm from the rail head center, so as to characterize the vertical rail wear positions of HSR more accurately.

Refer to Table 2 for the rail wear measuring points on 5 curve sections with different radius and straight sections of Beijing–Shanghai HRS and the corresponding kilometer posts and Figure 2 for the comparison between different rail wear rates. In Figure 2, U75VH heat-treated rails are laid at measuring point K2 and U71MnK hot-rolled rails are laid at other measuring points. According to Figure 2, when the curve radius is greater than 2,495 m, the wear rate of straight sections is basically the same as that of curve sections; the wear rates of the two curves with a radius of 460 m and 800 m are significantly greater, especially that of the curve with a radius of 460 m. Although U75VH heat-treated rails are used, the wear rate is about 1.5 times that of the curve with a radius of 800 m.

Table 2.
Curve radius R of wear
measuring point
curves and the
corresponding
kilometer posts

Kilometer post	Curve radius R /m	Kilometer post	Curve radius R /m
K2	460	K1313	4,505
K4	800	K1253	8,000
K1316	2,495	K1252	∞

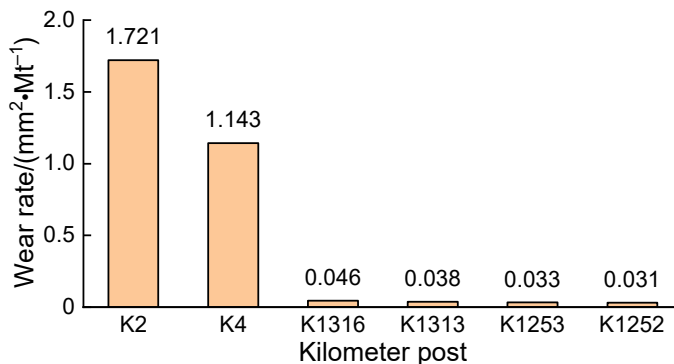


Figure 2.
Comparison between
rail wear rates on
different curve and
straight sections of
Beijing–Shanghai HSR

3. Changes in wheel profiles

One CRH380BL EMU train is selected from those serving Beijing–Shanghai HSR, one CRH380AL EMU train from those serving Wuhan–Guangzhou HSR, one CRH380BG EMU train from those serving Harbin–Dalian HSR, one CRH2G EMU train from those serving Lanzhou–Urumchi HSR, one CRH₂A EMU train from those serving Guiyang–Guangzhou HSR, and one CRH₅G EMU train from those serving Dandong–Dalian HSR for wheel wear analysis, and the results are shown in Figures 3–8.

It can be seen from Figure 3 that there is an approximate linear increase relationship between the wheel wear and the service mileage; when the service mileage reaches 205,000 km, the tread wear of all wheels of the entire train shows characteristics of normal distribution; the tread wear in a range from 0.6 to 0.7 mm accounts for 53.1%, and the maximum tread wear is about 0.9 mm; the wheel flanges are worn to a small extent, and the wear in the middle of the tread is distributed in a range from –25 to 30 mm.

It can be seen from Figure 4 that there is an approximate linear increase relationship between the wheel wear and the service mileage; the wheel wear of all wheels of the entire train is highly discrete: when the service mileage reaches 179,000 km, the tread wear in a range from 0.5 to 0.6 mm accounts for the largest part, i.e. 34.4%, and the maximum tread wear is about 0.8 mm; both the middle part of the tread and the wheel flange are worn and the wear in the middle of the tread is distributed in a range from –30 to 50 mm.

It can be seen from Figure 5 that the wheel wear increases with the increase of the service mileage; when the service mileage reaches 242,000 km, the tread wear of all wheels of the entire train shows the characteristics of normal distribution: the tread wear in a range from 1.0 to 1.1 mm accounts for the largest part, i.e. 51.6%, and the maximum tread wear is about 1.6 mm; the wear in the middle of the tread is distributed in a range from –30 to 35 mm.

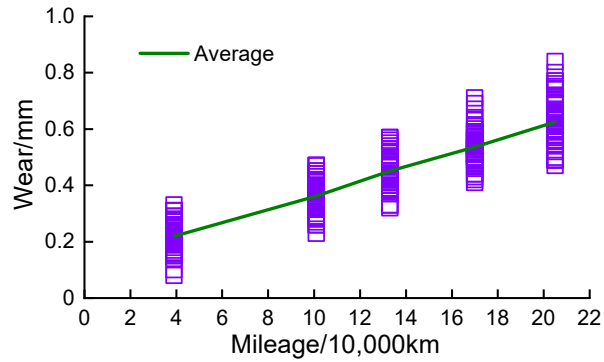
It can be seen from Figure 6 that the wheel wear gradually increases with the increase of the service mileage; when the service mileage reaches 242,000 km, the tread wear of all wheels of the entire train shows the characteristics of normal distribution: the tread wear in a range from 1.05 to 1.20 mm accounts for the largest part, i.e. 40.6%, and the maximum tread wear is about 1.5 mm; the wear mainly occurs in the middle of the tread and is distributed in a narrow range from –20 to 30 mm.

It can be seen from Figure 7 that the wheel wear gradually increases with the increase of the service mileage; when the service mileage reaches 218,000 km, the tread wear of all wheels of the entire train shows the characteristics of normal distribution: the tread wear in a range from 0.5 to 0.6 mm accounts for the largest part, i.e. 53.8%; the wear mainly occurs in tread and is distributed in a wide range, mainly from –35 to 50 mm on the abscissa axis.

It can be seen from Figure 8 that the wheel wear gradually increases with the increase of the service mileage, and wheel wear of all wheels of the entire train becomes more discrete while the service mileage increases; when the service mileage reaches 266,000 km, the tread wear of all the wheels is mainly distributed in a range from 1.05 to 1.20 mm (accounting for 23.4%) and from 1.20 to 1.35 mm (accounting for 20.3%); the maximum tread wear is about 1.95 mm; both the middle of the tread and the wheel flange are worn to a certain extent, and the wear in the middle of the tread is centralized in a range from –20 to 40 mm.

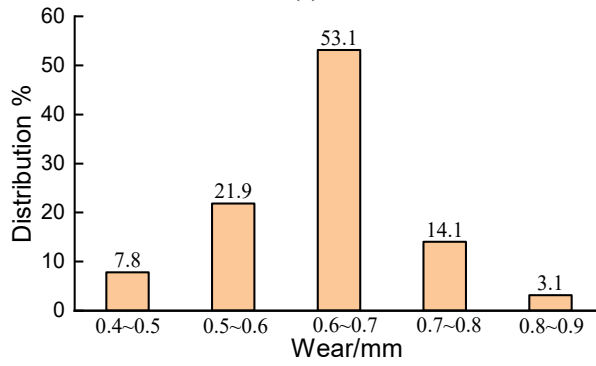
The tread wear rates of EMU trains running on the 6 lines above are calculated and the comparison results are shown in Figure 9.

It can be seen from Figure 9 that the tread wear rate of the trains on Dandong–Dalian HSR is the maximum, i.e. about $0.06 \text{ mm} \cdot (10,000 \text{ km})^{-1}$; that on Harbin–Dalian HSR and that on Lanzhou–Urumchi HSR are both about $0.05 \text{ mm} \cdot (10,000 \text{ km})^{-1}$; that on Beijing–Shanghai HSR and that on Wuhan–Guangzhou HSR are both about $0.035 \text{ mm} \cdot (10,000 \text{ km})^{-1}$; that on Guiyang–Guangzhou HSR is about $0.031 \text{ mm} \cdot (10,000 \text{ km})^{-1}$. Although track conditions, track excitation conditions, types of the trains, wheel and rail profiles and materials, and climate conditions are different, the wheel wear rates of trains on Harbin–Dalian, Lanzhou–



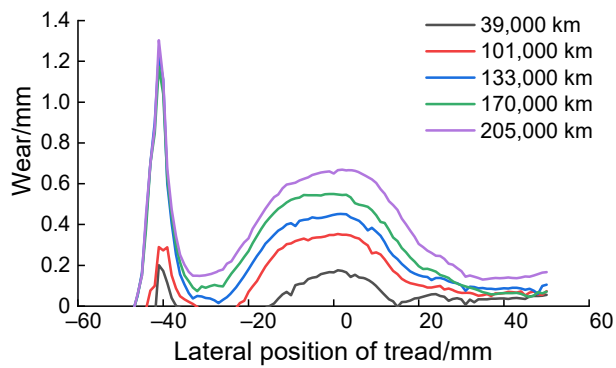
Tread wear changing with service mileage

(a)



Statistics of tread wear at the end of a reprofiling cycle

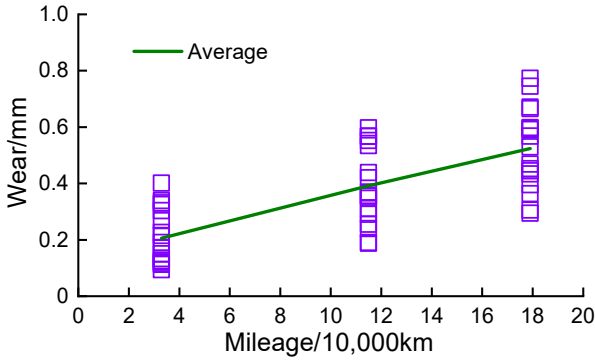
(b)



Typical tread wear distribution

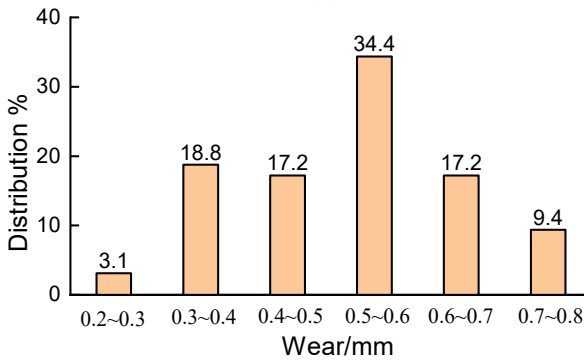
(c)

Figure 3.
Wheel wear of a
CRH380BL EMU train
on Beijing-
Shanghai HSR



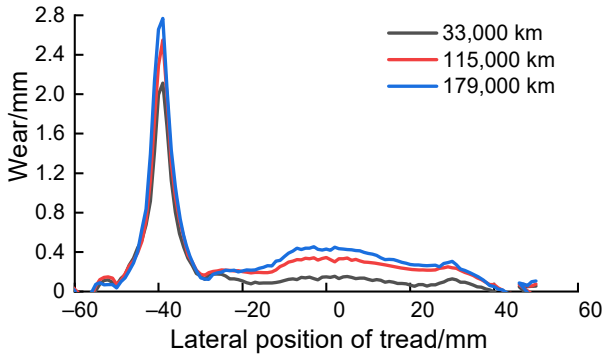
Tread wear changing with service mileage

(a)



Statistics of tread wear at the end of a reprofiling cycle

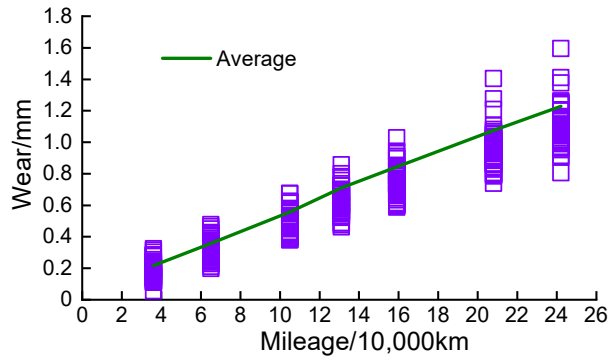
(b)



Typical tread wear distribution

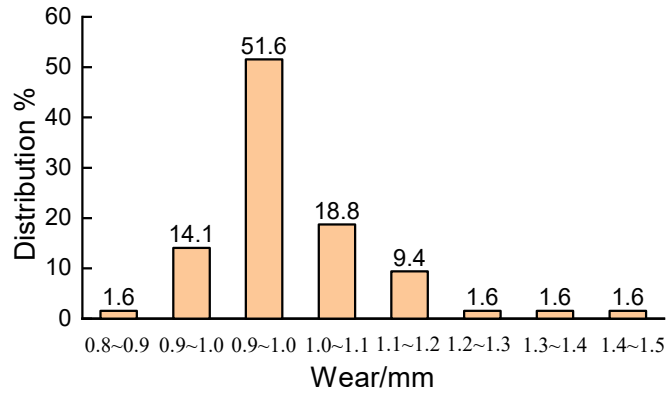
(c)

Figure 4.
Wheel wear of a
CRH380AL EMU train
on Wuhan–
Guangzhou HSR



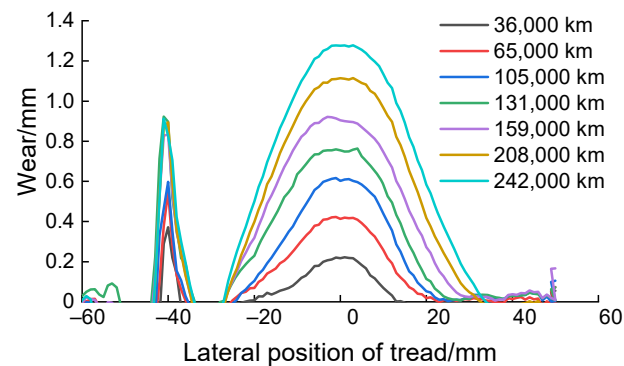
Tread wear changing with service mileage

(a)



Statistics of tread wear at the end of a reprofiling cycle

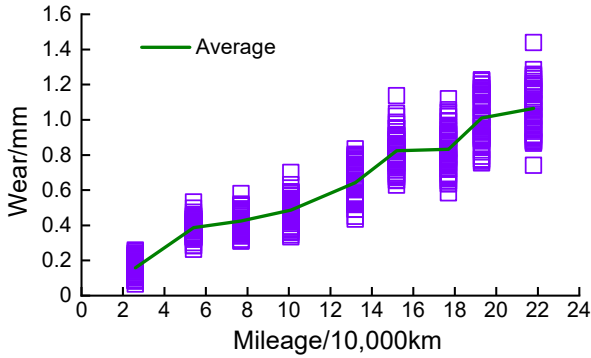
(b)



Typical tread wear distribution

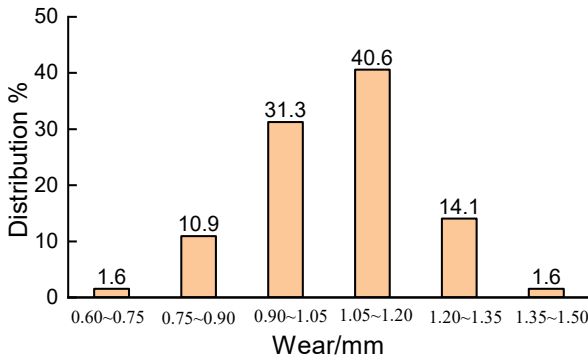
(c)

Figure 5.
Wheel wear of a
CRH380BG EMU train
on Harbin-Dalian HSR



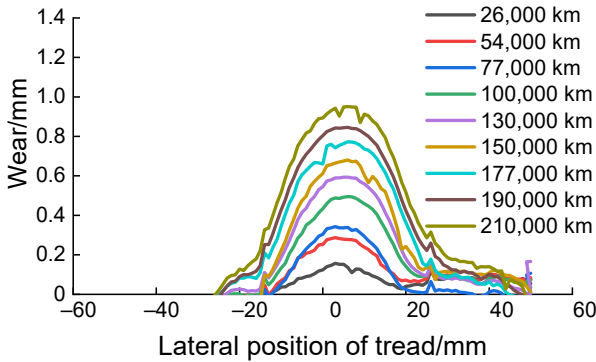
Tread wear changing with service mileage

(a)



Statistics of tread wear at the end of a reprofiling cycle

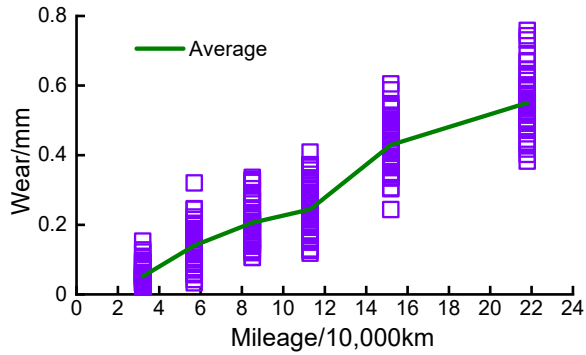
(b)



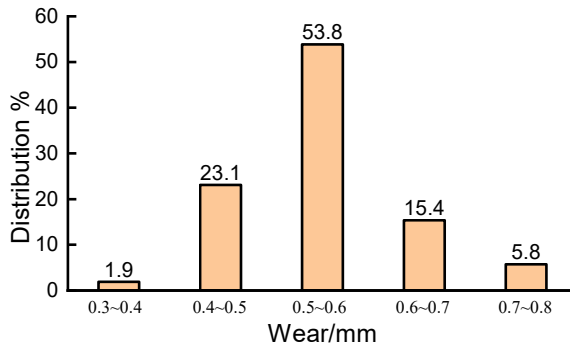
Typical tread wear distribution

(c)

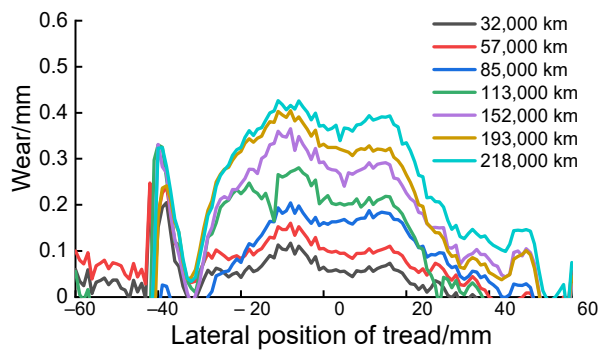
Figure 6.
Wheel wear of a
CRH₂G EMU train on
Lanzhou–
Urumchi HSR



Tread wear changing with service mileage
(a)

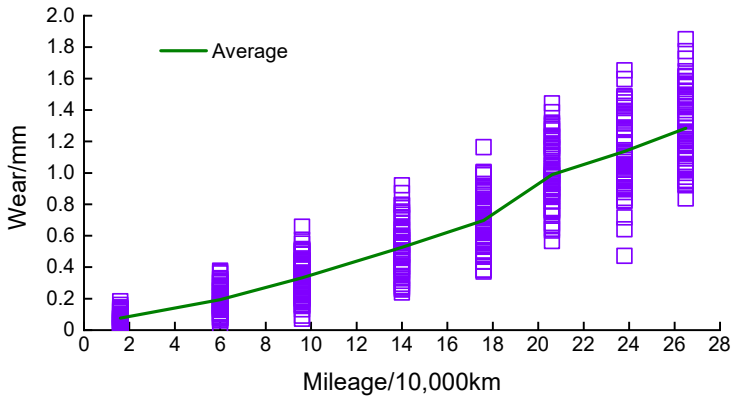


Statistics of tread wear at the end of a reprofiling cycle
(b)



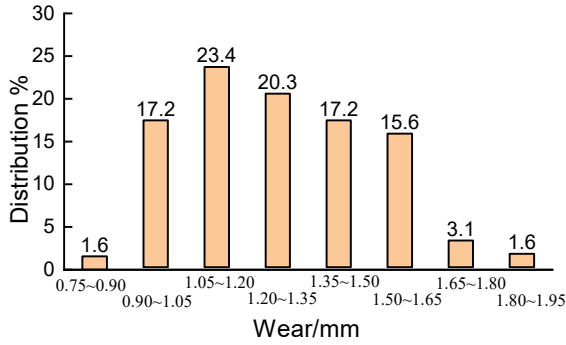
Typical tread wear distribution
(c)

Figure 7.
Wheel wear of a
CRH₂A EMU train on
Guiyang-
Guangzhou HSR



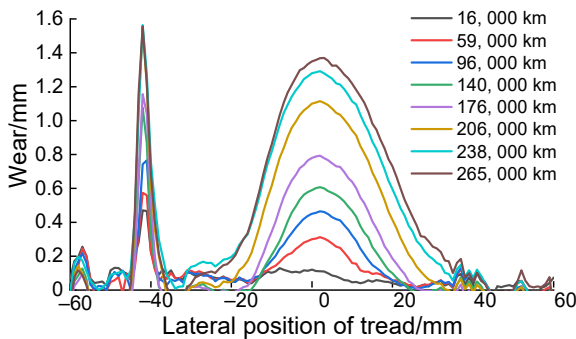
Tread wear changing with service mileage

(a)



Statistics of tread wear at the end of a reprofiling cycle

(b)



Typical tread wear distribution

(c)

Figure 8.
Wheel wear of a
CRH₅G EMU train on
Dandong–Dalian HSR

Urumchi and Dandong–Dalian HSR are high because these HSR are all in dry and sandstorm areas in northern China and the wheel–rail dynamic interaction is large due to the high wheel–rail friction coefficient. On the contrary, the wheel wear rates of trains on Beijing–Shanghai, Wuhan–Guangzhou and Guiyang–Guangzhou HSR are low because these HSR are all in wet areas in southern China, and the wheel–rail dynamic interaction is small and the wheel–rail wear coefficient is low.

Flange wear changing with tread wear of different trains is shown in Figure 10. According to Figure 10, the flange wear of the 6 trains is less than the tread wear; the flange wear of the trains on Lanzhou–Urumchi HSR is the minimum, basically less than 0.1 mm; the flange wear of the trains on Wuhan–Guangzhou HSR is greater than the tread wear, and when the flange wear is about 0.9 mm, the tread wear is about 0.5 mm; the flange wear of the rest 4 trains increases with the increase of the tread wear; the wear in the middle of the tread is greater than that of the flange, and the wear mainly occurs in the tread. The CRH380AL EMU train on Wuhan–Guangzhou HSR is allocated to CR-Wuhan, and the flange wear is relatively large due to the existence of curves with a radius ranging from 300 to 700 m at Wuhan Hub.

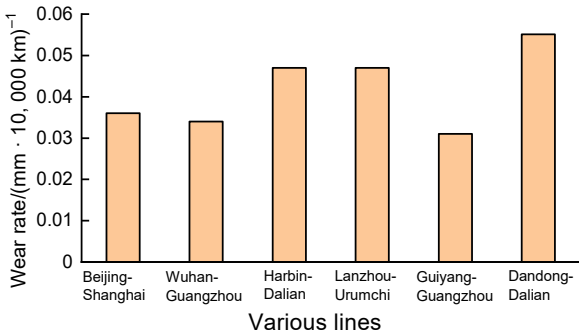


Figure 9.
Comparison between tread wear rates of trains running on various lines

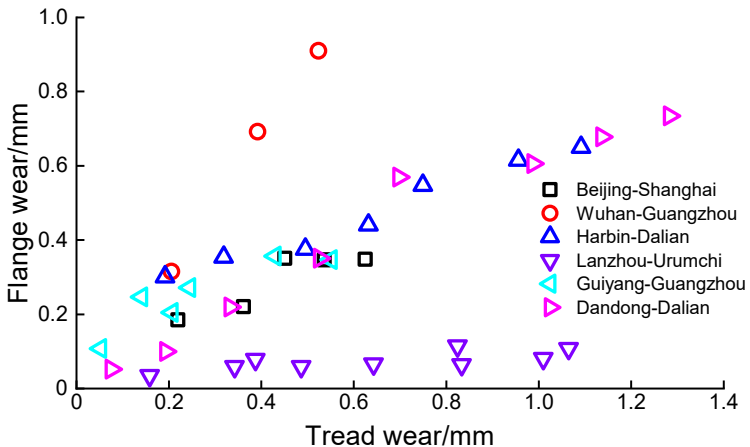


Figure 10.
Flange wear changing with tread wear of different trains

4. Matching characteristics of wheel and rail profiles

Three standard treads (LMA, S1002CN and XP55) are matched with TB60 and 60N rail profiles and the typical measured rail profiles of the 6 lines. Changes in the equivalent conicity are calculated and analyzed as shown in Figure 11.

According to Figure 11, the equivalent conicity of LMA, S1002CN and XP55 matched with the 8 rail profiles above is distributed in a range from 0.026 to 0.034, from 0.100 to 0.170, and from 0.053 to 0.057, respectively; LMA and XP55 treads are less affected by changes in rail profiles and the equivalent conicity basically remains stable. S1002CN tread is greatly affected by changes in rail profiles. For rail grinding of the 6 lines, the 60D pre-grinding profile is adopted. However, grinding processes and methods used by different work teams are not the same, making the measured 60D rail profiles on different sections of these lines are different, and thus the equivalent conicity of S1002CN tread matched with the measured rail profiles of some lines decreases to 0.09, resulting in lurching at a low conicity, i.e. secondary sinuation instability and affecting the ride comfort.

The equivalent conicity is calculated through the matching between the measured wheel profiles within one reprofiling cycle of the 6 trains above and each measured rail profile of the lines, and the average wear and average equivalent conicity are worked out by calculations on 64 wheels of 8 cars. The changes in average wheel wear and average equivalent conicity within one reprofiling cycle with the increase of service mileage are shown in Figure 12. According to Figure 12, the average equivalent conicity within one reprofiling cycle of the wheels of the CRH₂A EMU trains on Guiyang–Guangzhou HSR basically remains stable around 0.03, and it does not change significantly with the increase of the average tread wear; the average equivalent conicity of the CRH380AL EMU trains on Wuhan–Guangzhou HSR decreases with the increase of the average tread wear and the equivalent conicity decreases from 0.045 at the beginning of one reprofiling cycle to 0.025 at the end of the cycle; the average equivalent conicity of the rest four lines all increases with the increase of the average tread wear: the average equivalent conicity at the end of a reprofiling cycle of the CRH380BL trains on Beijing–Shanghai HSR is 0.36, that of the CRH380BG trains on Harbin–Dalian HSR is 0.32, that of the CRH₂G trains on Lanzhou–Urumchi HSR is 0.19 and that of the CRH₅G trains on Dandong–Dalian HSR is 0.23.

According to the analysis above, the wheel wear of the two trains, i.e. CRH380AL on Wuhan–Guangzhou HSR and CRH₂A on Guiyang–Guangzhou HSR is distributed in a

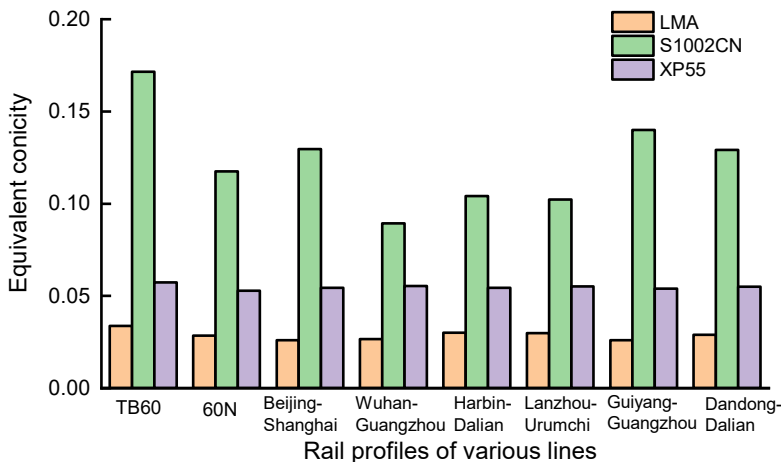
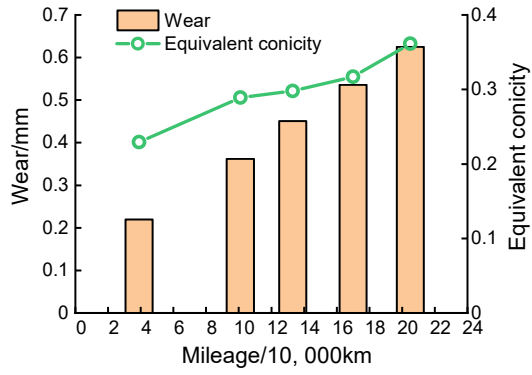
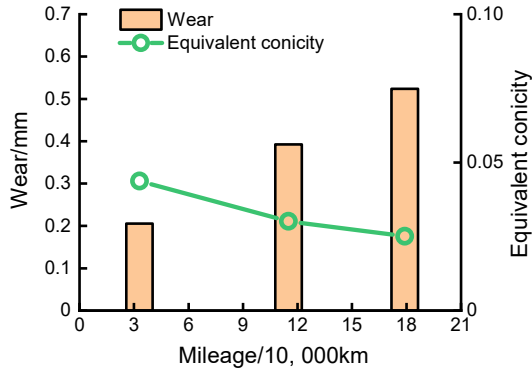


Figure 11. Changes in equivalent conicity of 3 wheel treads matched with different rail profiles



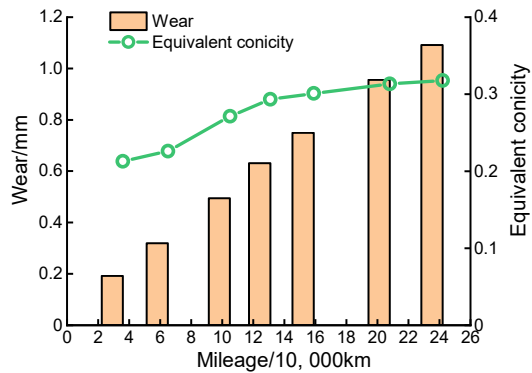
Beijing-Shanghai HSR

(a)



Wuhan-Guangzhou HSR

(b)

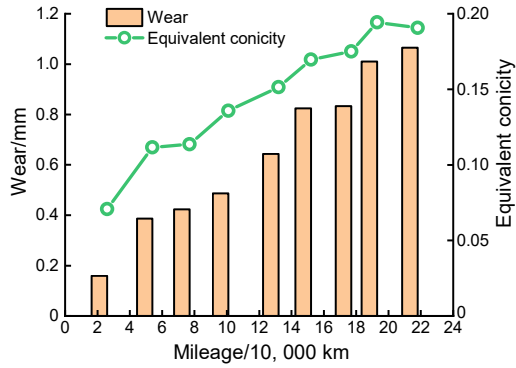


Harbin-Dalian HSR

(c)

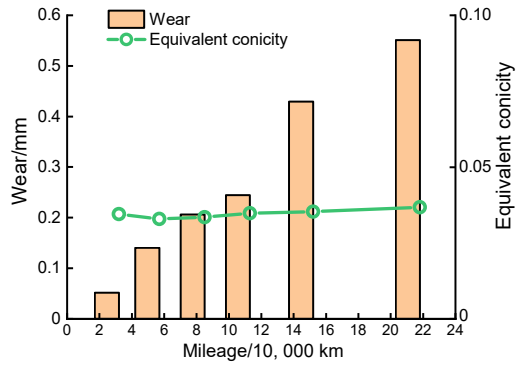
Figure 12. Average wheel wear in one reprofiling cycle of various trains and the corresponding equivalent concity

(continued)



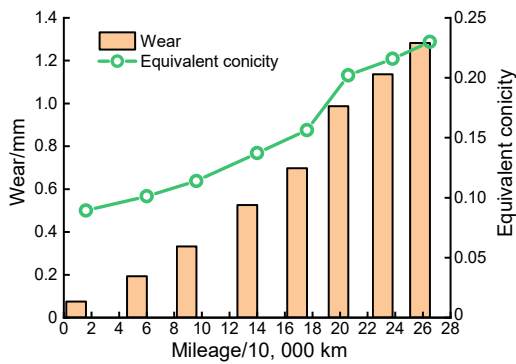
Lanzhou-Urumchi HSR

(d)



Guiyang-Guangzhou HSR

(e)



Dandong-Dalian HSR

(f)

Figure 12.

relatively wide range, the tread wear is distributed in a range from -30 to 50 mm, and the wheel–rail contact is uniform, making the equivalent conicity do not increase significantly; the wheel wear of the rest 4 trains is distributed in a narrow range generally from -25 to 30 mm, the wheel–rail contact is relatively concentrated, and as a result hollow wear usually occurs and the equivalent conicity increases quickly.

The equivalent conicity of matching between wheel and rail profiles should be controlled within a reasonable range. Hollow tread wear makes the equivalent conicity increase rapidly. An equivalent conicity exceeding the limit often triggers the alarm for lateral vibration acceleration of high speed car frames, which affects the normal and safe railway transport; however, a too small equivalent conicity often causes the low-frequency lateral lurching of cars, which enlarge the riding index and reduces the ride comfort. The equivalent conicity of wheels of the CRH380AL EMU trains on Wuhan–Guangzhou HSR and that of the CRH₂A EMUs on Guiyang–Guangzhou HSR do not increase with the increase of the tread wear, which is conducive to extending the wheel reprofiling cycle. Meanwhile, attention should be paid to the risk of low conicity of wheels of the CRH380AL EMU trains on Wuhan–Guangzhou HSR caused by its continuous decrease.

5. Conclusions

This paper analyzes the change rules in rail profiles and wheel profiles of various lines with a modern statistical method. Additionally, in this way, the main characteristics of the equivalent conicity matching and the difference between various HSR in China are obtained and relevant optimization measures and suggestions are proposed.

- (1) The natural rail wear of HSR main lines remains very little. For the lines with an annual passing tonnage of less than 11 Mt, the vertical rail wear is less than 0.01 mm, which is beyond the measuring precision of instruments for the moment. The changes in rail profiles caused by rail grinding are obvious, at most accounting for about 90% of the profile change rules. The maximum wear points of 68.4% of profile area changes are concentrated in a range from 0 to 5 mm from the rail head center to the working gauge. Therefore, it is recommended to measure the vertical wear at 5 mm from the rail head center, so as to fully reflect the characteristics of the vertical rail wear of HSR. When the radius of a curve section is greater than 2,495 m, the rail wear rates on the straight section and the curve section are basically the same. The rail wear rate on the curve section with a radius of less than 800 m is much higher.
- (2) In one wheel reprofiling cycle, the tread wear gradually increases with the increase of service mileage, and the tread wear of all the wheels of the entire train represents the characteristics of normal distribution, and the tread wear gradually becomes more discrete while the service mileage increases. The tread wear of the trains on Harbin–Dalian, Lanzhou–Urumchi and Dandong–Dalian HSR is relatively large, and the average tread wear rate is about $0.05\text{--}0.06 \text{ mm} \cdot (10,000 \text{ km})^{-1}$. The average tread wear rate of trains on Beijing–Shanghai, Wuhan–Guangzhou and Guiyang–Guangzhou HSR is $0.03\text{--}0.035 \text{ mm} \cdot (10,000 \text{ km})^{-1}$.
- (3) Except that the flange wear of a few trains is relatively large, the wheel wear of other trains is mostly the tread wear. The tread wear of the CRH380AL EMU trains on Wuhan–Guangzhou HSR and the CRH₂A trains on Guiyang–Guangzhou HSR is distributed in a wide range from -30 to 50 mm while the tread wear of other trains is distributed in a narrow range generally from -25 to 30 mm.
- (4) Among the 3 types of wheel tread, i.e. LMA, S1002CN and XP55, S1002CN wheel profile is usually affected by changes in rail profiles and LMA and XP55 wheel

profiles are less affected by such changes. The rail profiles measured on HSR in China are quite different from TB60 profile, and they mainly include 60D pre-grinding profile and 60N profile. However, different grinding processes and methods are used on site, and rail profiles on different sections are different. Therefore, it is necessary to strictly control the rail profile deviation and determine the grinding deviation range. For tread optimization or analysis on dynamic behaviors of cars, the characteristics of measured rail profiles should be taken into consideration while TB60 rail profile should not be used as the reference profile.

- (5) Changes in equivalent conicity is analyzed by matching measured wheel profiles with measured rail profiles. In one reprofiling cycle, the equivalent conicity of the wheels of the CRH380AL EMU trains on Wuhan–Guangzhou HSR and that of the CRH2A EMU trains on Guiyang–Guangzhou HSR do not increase significantly, and the equivalent conicity of the wheels of the rest 4 trains increases with the increase of the tread wear. This is because the wheel wear range of the trains on Wuhan–Guangzhou HSR and the trains on Guiyang–Guangzhou HSR is wide, the wheel–rail contact points are evenly distributed, hollow wear rarely occurs, the equivalent conicity changes slowly, and all these factors are conducive to extending the wheel reprofiling cycle. Meanwhile, further attention should be paid to the risk of low conicity of wheels of the trains on Wuhan–Guangzhou HSR caused by its continuous decrease. According to the field test, this paper proposes the distribution range of the equivalent conicity in one reprofiling cycle of various EMU trains, which provides guidance for the condition-based wheel reprofiling.

References

- Dong, X., Wang, Y., Ren, Z., Wang, L., & Liu, H. (2014). Design and application of thin flange wheel tread profiles for CRH3C EMUs. *Journal of the China Railway Society*, 36(2), 11–17.
- Gan, F., Dai, H., Gao, H., & Wei, L. (2013). Calculation of equivalent conicity and wheel-rail contact relationship of different railway vehicle tread. *Journal of the China Railway Society*, 35(9), 19–24.
- Hou, M., Fang, X., Chang, C., Hu, X., Liu, F., Dong, X., Wang, S., Tu, Y., & Guo, T. (2018). Design and study of field test of HSR wheel-rail interaction. *Chinese Railways*, (1), 30–35.
- Huang, Z., Cui, D., Du, X., & Jin, X. (2013). Influence of deviated wear of wheel on performance of high-speed train running on straight tracks. *Journal of the China Railway Society*, 35(2), 14–20.
- Jin, X., Zhao, G., Liang, S., Tao, G., Cui, D., & Wen, Z. (2018). Characteristics, mechanisms, influences and counter measures of high speed wheel/rail wear: Transverse wear of wheel tread. *Chinese Journal of Mechanical Engineering*, 54(4), 3–14.
- Karttunen, K., Kabo, E., & Ekberg, A. (2014). Numerical assessment of the influence of worn wheel thread geometry on rail and wheel deterioration. *Wear*, 317(1/2), 77–91.
- Li, X., Wen, Z., & Jin, X. (2008). Effect of rail cant on the rolling contact behaviour of LM and LMA wheelsets. *Chinese Journal of Mechanical Engineering*, 44(3), 64–69.
- National Railway Administration of the People's Republic of China (2018). *TY [2012] No. 83 Rules on Maintenance of Ballastless Track of High Speed Railway (Temporary)*. Beijing: China Railway Publishing House.
- Polach, O. (2010). Characteristic parameters of nonlinear wheel/rail contact geometry. *Vehicle System Dynamics*, 48(1), 19–36.
- Sawlyw, K., & Wu, H. (2005). The formation of hollow-worn wheels and their effect on wheel/rail interaction. *Wear*, 258(7/8), 1179–1186.
- Sun, L. (2017). Influence of wheel-rail profile matching for high speed railway on vehicle dynamics performance. *China Railway Science*, 38(6), 108–117.

-
- Sun, S., Wang, C., Li, H., & Zeng, S. (2006). Analysis of wheel/rail contact geometric parameters' effect on the dynamic behavior of high-speed passenger car. *China Railway Science*, 27(5), 93–98.
- Wu, H., Kalay, S., & Tournay, H. (2011). Development of the wheel-rail interface management model and its applications in heavy haul operations. *Proceedings of the Institution of Mechanical Engineers, Part F: Journal of Rail and Rapid Transit*, 225, 38–47.
- Zhang, J., Xiao, X., Wang, Y., & Jin, X. (2009). Comparison of characteristics of three high-speed wheelset profiles. *Journal of the China Railway Society*, 31(2), 23–31.
- Zhang, J., Jin, X., Sun, L., & Zhang, J. (2010). Preliminary research on the relationship between wheelset dynamic performance and equivalent conicity based on CRH₅ high-speed EMU vehicles. *Journal of the China Railway Society*, 32(3), 20–27.
- Zhou, Q., Tian, C., Zhang, Y., Chang, C., & Hou, M. (2014a). Cause analysis for the lateral instability of CRH₃ EMU framework. *China Railway Science*, 35(6), 105–110.
- Zhou, Q., Zhang, Y., Tian, C., Chen, C., Fiu, F., Yu, Z., & Li, L. (2014b). Profile design and test study of 60N Rail. *China Railway Science*, 35(2), 128–135.
- Zhou, Q., Liu, F., Zhang, Y., Tian, C., Yu, Z., & Zhang, J. (2017). Solution for problems at wheel-rail interface in high speed railway. *China Railway Science*, 38(5), 78–84.

Corresponding author

Maorui Hou can be contacted at: houmaorui@126.com